



Rescue of the Congenital Hereditary Endothelial Dystrophy Mouse Model by Adeno-Associated Virus–Mediated *Slc4a11* Replacement

Rajalekshmy Shyam, PhD, Diego G. Ogando, PhD, Edward T. Kim, BS, Subashree Murugan, BOptom, Moonjung Choi, PhD, Joseph A. Bonanno, OD, PhD

Purpose: Congenital hereditary endothelial dystrophy (CHED) is a rare condition that manifests at an early age showing corneal edema, increased oxidative stress, mitochondrial dysfunction, and eventually apoptosis of the endothelium due to loss of function of the membrane transport protein SLC4A11. This project tested whether replacing *Slc4a11* into the *Slc4a11*^{-/-} CHED mouse model can reverse the disease-associated phenotypes.

Design: Experimental study.

Participants: Five-week-old or 11-week-old *Slc4a11*^{-/-} mice. Age- and gender-matched *Slc4a11*^{+/+} animals were used as controls. A total of 124 animals (62 female, and 62 male) were used in this study. Fifty-three animals of the genotype *Slc4a11*^{+/+} were used as age- and gender-matched noninjected controls. Seventy-one *Slc4a11*^{-/-} mice were administered anterior chamber injections of adeno-associated virus (AAV).

Methods: Anterior chambers of young (5 weeks old) or older (11 weeks old) *Slc4a11*^{-/-} mice were injected once with adeno-associated virus serotype 9 (AAV9) mouse *Slc4a11* or AAV9-Null vectors. Corneal thickness was measured using OCT. End point analysis included corneal endothelial cell density, mitochondrial oxidative stress, and corneal lactate concentration.

Main Outcome Measures: Corneal thickness, endothelial cell loss, lactate levels, and mitochondrial oxidative stress.

Results: In the young animals, AAV9-*Slc4a11* reversed corneal edema, endothelial cell loss, mitochondrial oxidative stress, lactate transporter expression, and corneal lactate concentration to the levels observed in wild-type animals. In the older animals, gene replacement did not reverse the phenotype but prevented progression.

Conclusions: Functional rescue of CHED phenotypes in the *Slc4a11*^{-/-} mouse is possible; however, early intervention is critical. *Ophthalmology Science* 2022;2:100084 © 2021 by the American Academy of Ophthalmology. This is an open access article under the CC BY-NC-ND license (<http://creativecommons.org/licenses/by-nc-nd/4.0/>).



Supplemental material available at www.ophtalmologyscience.org.

The corneal endothelium is a single layer of nonproliferating cells that line the posterior side of the cornea.^{1,2} These cells maintain corneal transparency through an active pump mechanism that moves water linked to lactate transport across the endothelium from the stroma into the aqueous humor, thereby requiring an intact osmotic barrier.^{1,2} Congenital hereditary endothelial dystrophy (CHED) is a rare recessive condition that affects 3 of 100 000 newborns each year,^{2,3} leading to bilateral corneal edema and clouding.^{4–7} Mutations in *Slc4a11*, which codes for a plasma membrane H⁺ transporter and an ammonia sensitive mitochondrial uncoupler,⁶ lead to CHED.⁴ *Slc4a11*^{-/-} (knockout [KO]) mice recapitulate the progressive corneal edema, endothelial cell loss, and corneal opacity, seen in the disease phenotype^{4,5,8} along with a loss of lactate transporters and accumulation of stromal lactate.^{9,10} The

only treatment available for CHED is corneal transplantation.^{8,11} This invasive procedure also presents challenges because of the scarcity of donor tissue, graft rejection, and the need for prolonged postsurgical management.^{12–14}

A potential treatment avenue not explored in CHED and other corneal endothelial dystrophies is gene therapy. This method has had some success in retinal diseases and glaucoma.^{15,16} Recently, adenovirus-mediated CRISPR/Cas9 knockdown of mutant Collagen 8a2 showed functional rescue of disease phenotype associated with early-onset Fuchs' endothelial corneal dystrophy.¹⁷ In the current study, we asked if gene therapy can reverse the disease-associated phenotype in CHED. Anterior chamber injection of adeno-associated virus serotype 9 (AAV9) with hemagglutinin (HA) tagged mouse *Slc4a11* into *Slc4a11*^{-/-} mice

rescued the major disease phenotype, including corneal edema, stromal [lactate], and corneal endothelial cell death. Also, we show that time of intervention is crucial for altering disease progression. Delivery of AAV9-*HA-Slc4a11* in young mice produced some reversal of the disease, whereas in the older animals, gene replacement did not reverse the disease course but prevented progression.

Methods

Adeno-Associated Virus

Adeno-associated virus serotype 9-CAG-*HA-Slc4a11* delivered mouse *Slc4a11* cDNA with HA-tag at the N-terminus under the control of chicken β -actin (CAG) promoter via anterior chamber injections. The AAV9-CAG-null, which contained AAV9 capsid, CAG promoter but no transgene, was used as negative control. Both these vectors were custom produced by Vector Biolabs. The AAV9-CAG-green fluorescent protein (GFP) (#37825) was purchased from Addgene.

Animal Housing, Maintenance, and Anterior Chamber Injections

Slc4a11^{+/+} (wild-type [WT]) and *Slc4a11*^{-/-} mice were housed and maintained in pathogen-free conditions. All animal experiments were conducted in accordance with institutional guidelines and the current regulations of the National Institutes of Health, the US Department of Health and Human Services, the US Department of Agriculture, and the Association for Research in Vision and Ophthalmology Statement for the Use of Animals in Ophthalmic and Vision Research. *Slc4a11* KO mice were created with a targeted deletion of exons 9–13 of the mouse *Slc4a11* gene. These animals are in C57BL6 background and were a gift from Professor Eranga Vithana (Singapore National Eye Center).

Mice were anesthetized using intraperitoneal injections of ketamine, 100 mg/kg, and xylazine, 10 mg/kg. Eyes were dilated with phenylephrine hydrochloride solution (#847287, Paragon Bio Teck) and anesthetized using Proparacaine (Bausch & Lomb). With the use of a 34-gauge needle attached to a micro-manipulator (#M3301-M3-R, WPI Instruments), anterior chamber injection was conducted with the aid of microinjection syringe pump (#MICRO2T, WPI Instruments). A range of adeno-associated virus (AAV) doses from 9×10^8 GC/ μ l to 1×10^{12} GC/ μ l were previously shown to effectively transduce mouse corneal endothelium.¹⁸ Therefore, we chose to inject 0.5 μ l to 0.8 μ l of the solution containing diluted virus ($\sim 1.0 \times 10^{12}$ GC/ μ l) and 0.1% fluorescein, to aid visualization, once into the anterior chamber of the mouse eye. One eye was injected and the other was not injected in all experiments. For negative controls, 11-week-old *Slc4a11*^{-/-} animals were injected in 1 eye with 0.5–0.8 μ l AAV9-CAG-Null virus (0.9×10^{12} GC/ μ l). The AAV9 serotype transduction efficiency into the corneal endothelium was determined by the injection of 0.5 μ l AAV9-GFP (3.5×10^9 Viral Genome) into the anterior chamber of 11-week-old *Slc4a11*^{-/-} animals. A total of 124 animals (62 female and 62 male) were used in this study. Fifty-three animals of the genotype *Slc4a11*^{+/+} were used as age- and gender-matched noninjected controls. Seventy-one *Slc4a11*^{-/-} mice were subjected to anterior chamber injections of AAV.

Young animals were injected at 5 weeks of age and euthanized at 9 weeks of age. Older animals were injected at 11 weeks of age and euthanized at 15 weeks of age.

Slit-Lamp Microscopy

Anterior flare assessments were conducted using slit-lamp microscopy on 11-week-old *Slc4a11*^{-/-} animals injected with AAV-GFP. The slit-lamp user was blinded to the experimental conditions. Two male animals and 1 female animal (N = 3) were used.

Immunohistochemistry

Corneas were dissected and fixed in 4% paraformaldehyde for 10 minutes at room temperature. After permeabilizing the samples using 0.5% TritonX-100 and blocking in 5% donkey serum (#017-000-121, Jackson Immunologicals), primary antibody incubation of zonula occludens 1 (ZO-1) (#33-9100, Thermo Fisher Scientific, 1:100) or GFP (#2555, Cell Signaling Technologies) was carried out overnight at 4°C in the blocking buffer. Corneas were then washed in phosphate-buffered saline (PBS) and incubated in secondary antibodies for 1 hour at room temperature. Hoescht dye (1 μ m, #H3570, Thermo Fisher Scientific) was added to label the nuclei, and the tissues were mounted using Prolong Gold Anti-fade reagent (#P36934, Thermo Fisher Scientific). F-actin staining was conducted using Alexa Fluor 488 Phalloidin (#A12379, Thermo Fisher Scientific) following manufacturer's instructions and examined by Zeiss LSM 800 confocal microscope (Zeiss). Fluorescence intensity for phalloidin staining and cell area measurements were performed as described previously.⁹ Two female animals and 1 male animal per group per staining condition were used. Six animals were used for phalloidin staining, and 6 animals were used for ZO-1 staining.

Wes Immunoassay

Corneas were dissected and the endothelial cell layer was removed by peeling Descemet's membrane with jeweler's forceps. Protein lysates from corneal endothelial layers were extracted using RIPA lysis buffer (20188, Millipore Sigma) containing protease and phosphatase inhibitors. Protein lysates (1–3 μ g) were loaded into a 12–230 kDa separation module kit and analyzed using the Protein Simple Wes System (Protein Simple). Wes data were obtained as virtual blots in which the molecular weight and signal intensity along with electropherograms were presented. Antibodies and dilutions are as follows: monocarboxylate transporter (MCT)1 (Santa Cruz Biotechnologies, #sc365501, 1:10), MCT2 (Santa Cruz Biotechnologies, #sc166925, 1:10), MCT4 (Ab Clonal, #A10548, 1:10), superoxide dismutase 2 (Cell Signaling Technologies, #13141, 1:10), and α -Tubulin (Novus Biologicals, #NB100-690, 1:50). There were 3 young animals (2 female and 1 male) for each group. The total number of young animals used for this experiment was 6. There were 5 older animals (2 male and 1 female) for each group. The total number of older animals used for this experiment was 6. To determine transduction efficiency, we used HA antibody (#3724, Cell Signaling Technologies, 1:10). Three young animals (2 female and 1 male) per group were used. Three older animals (2 male and 1 female animal) per group were used.

Paraffin Sections and Immunostaining

For paraffin sectioning, enucleated eyes were fixed in 4% paraformaldehyde (Thermo Fisher Scientific, #28908) in 1 \times PBS at 4°C overnight, followed by dehydration in graded ethanol series (50%, 75%, 95%, 100%). The dehydrated eyes were immersed in paraffin overnight and then embedded. Sections 5- μ m thick were cut using a microtome (Leica Biosystems) after 24 hours. The sections were de-paraffinized, rehydrated in ethanol, and used for immunofluorescence staining. Antigen retrieval was performed by boiling the slides in sodium citrate buffer (10 mM sodium citrate, pH 6.0) and maintaining at sub-boiling temperature for 10 minutes. The slides were washed in ddH₂O for 5 minutes and blocked with

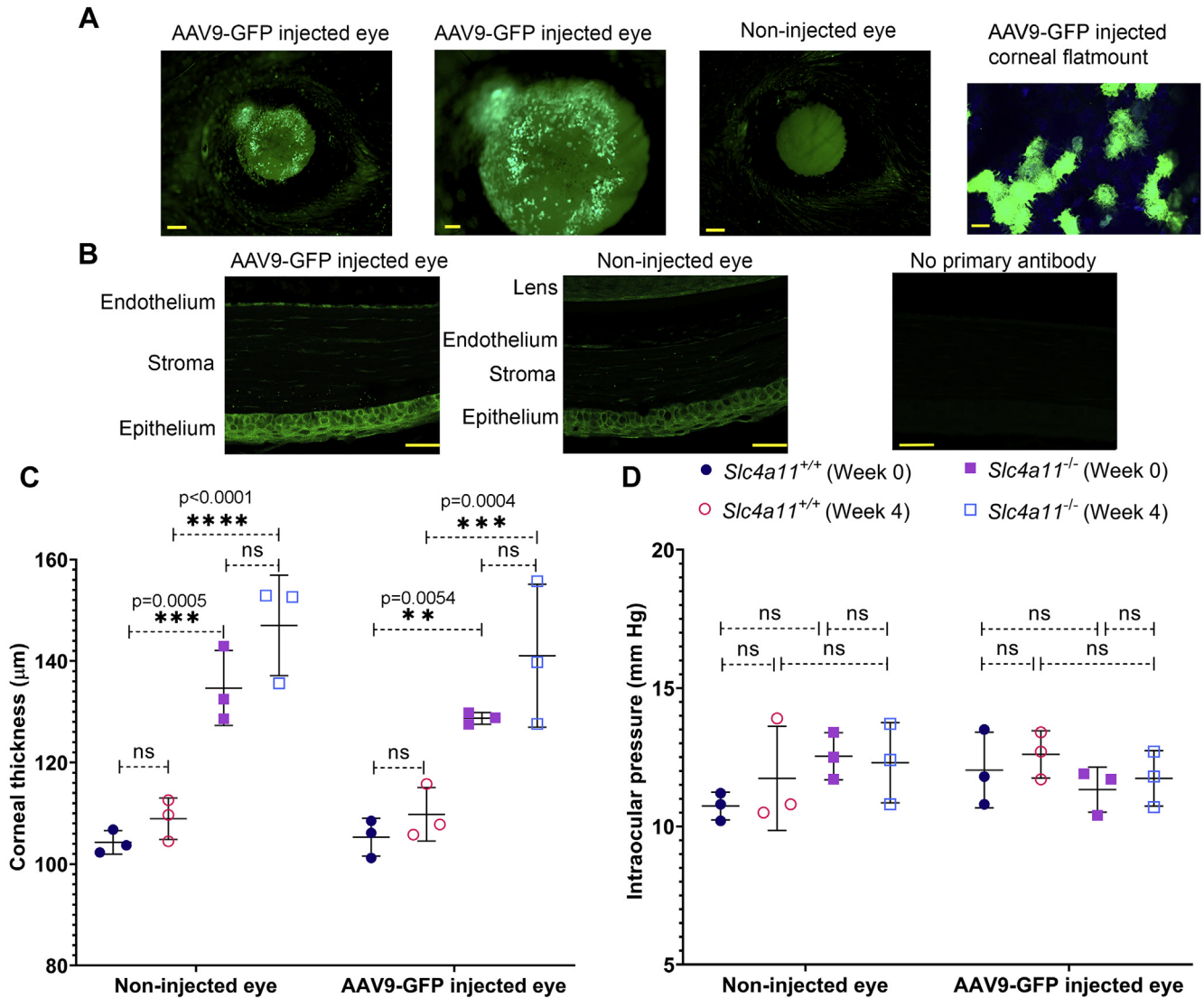


Figure 1. Adeno-associated virus serotype 9 green fluorescent protein (AAV9-GFP) is transduced into the corneal endothelium. **A**, Fluorescence microscopy of mouse eye 2 weeks after AAV9-GFP injection. Note endothelial fluorescence over a uniform background of lens fluorescence. Scale bar –500 μm (left and right images) and 200 μm (middle image). Flat mount of the cornea after GFP antibody staining in green and DAPI in Blue. Scale bar –20 μm . **B**, Cross-section of AAV9-GFP injected and noninjected eyes stained with GFP antibody. No primary antibody sections were only treated with secondary antibody. Scale bar –20 μm . **C**, Corneal thickness measurements of *Slc4a11*^{+/+} and *Slc4a11*^{-/-} animals before and 4 weeks after AAV9-GFP injections. Noninjected eyes of the same animals were used as control. **D**, Intraocular pressure measurements of *Slc4a11*^{+/+} and *Slc4a11*^{-/-} animals before and 4 weeks after AAV9-GFP injections. Noninjected eyes of the same animals were used as control: n = 3 (2 male and 1 female) per group for a total of 6 animals. ns = not significant, $P \geq 0.1$ (1-way analysis of variance [ANOVA] with Tukey’s multiple comparisons test).

5% donkey serum in 1 × PBST (PBS+0.1% Tween-20) for 30 minutes, then incubated overnight at 4 °C with the Anti-GFP antibody (# ab290, Abcam) at 1:50 dilution in the blocking buffer. After 3 washes in 1 × PBST, the slides were incubated for 1 hour at room temperature with secondary antibody. The slides were washed again and mounted with Fluoromount G mounting medium (Thermo Scientific, #00-4958-02) and examined by Zeiss LSM 800 confocal microscope (Zeiss). A total of 3 (2 male and 1 female) animals were used.

OCT Measurements

Corneal cross-section images were obtained using iVue OCT (Optovue). Corneal thickness measurements were conducted before

anterior chamber injections (week 0), 2 weeks after the injection (week 2) and 1 month after the injection (week 4). All measurements were made at the same time of day. At least 3 measurements were made for each eye and averaged. The OCT operator was blinded to the experimental condition. For young animals, 2 male and 1 female *Slc4a11*^{+/+} and 2 male and 2 female *Slc4a11*^{-/-} animals were used for a total number of 7 young animals. For older animals, 2 male and 1 female *Slc4a11*^{+/+} and 3 male and 3 female *Slc4a11*^{-/-} animals were used for a total number of 9 older animals.

Lactate Assay

The cornea was dissected, and the epithelium and endothelium were removed. Stroma was placed in preweighed microcentrifuge

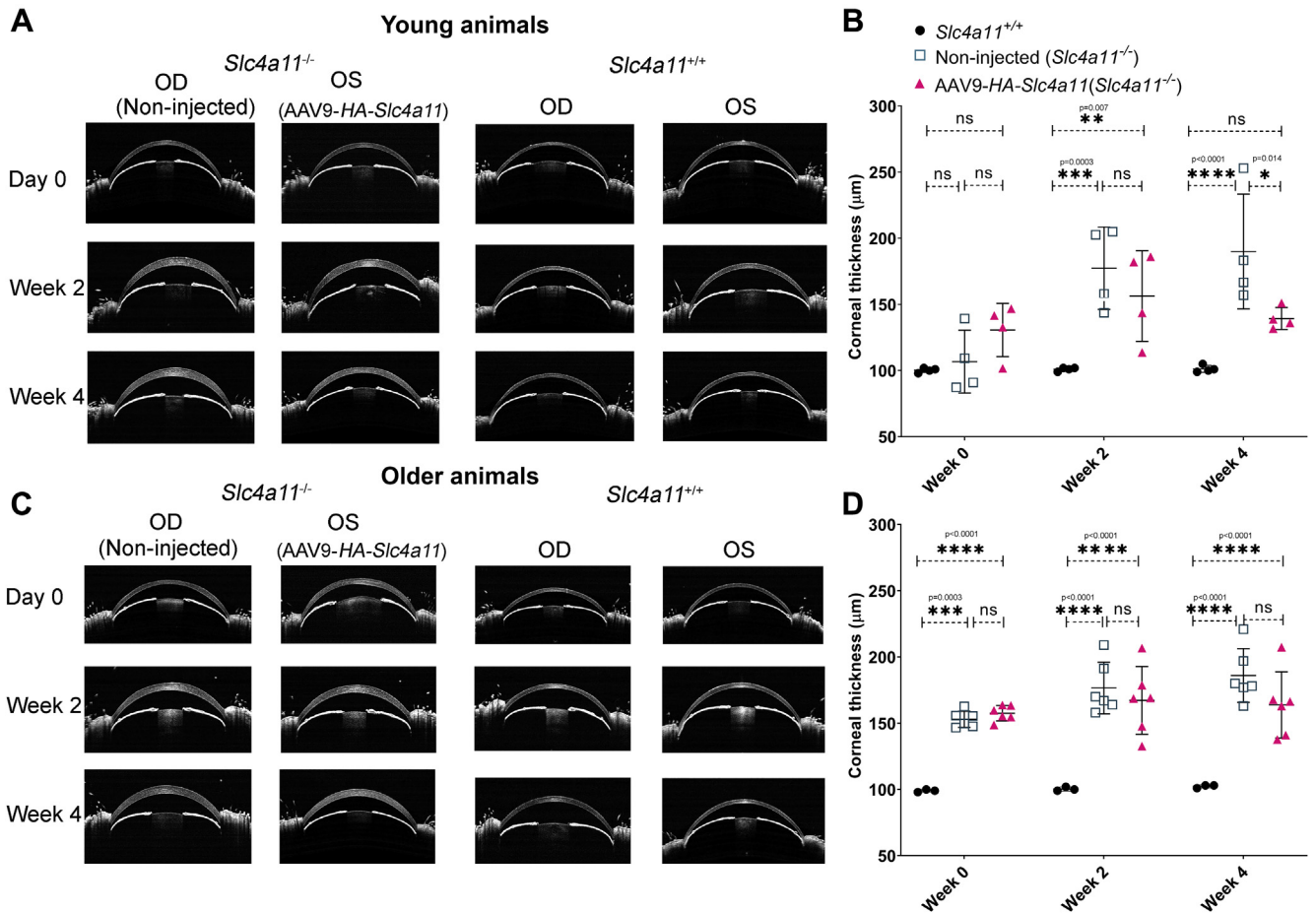


Figure 2. Corneal edema is reduced with AAV9-HA-*Slc4a11*. **A**, Representative OCT images of *Slc4a11*^{+/+}, noninjected *Slc4a11*^{-/-}, and AAV9-HA-*Slc4a11* injected *Slc4a11*^{-/-} eyes from young animals. **B**, Quantification of data from **A** (n = 4, 2 male and 2 female *Slc4a11*^{+/+}, 2 male and 2 female *Slc4a11*^{-/-} animals were used). **C**, Representative OCT images of *Slc4a11*^{+/+}, noninjected *Slc4a11*^{-/-}, and AAV9-HA-*Slc4a11* injected *Slc4a11*^{-/-} eyes from older animals (n = 3–6, 2 male and 1 female *Slc4a11*^{+/+}, 3 male and 3 female *Slc4a11*^{-/-} animals were used). **D**, Quantification of data from **C**. Mean ± standard deviation (SD). ns = not significant, P ≥ 0.1 (1-way ANOVA with Tukey’s multiple comparisons test). AAV9-HA = adeno-associated virus serotype 9 hemagglutinin; OD = right eye; OS = left eye.

tubes, crushed in liquid nitrogen, and homogenized in PBS. The sample was centrifuged at 15000g for 15 minutes at 4°C, and the supernatant was removed. Lactate was measured in the supernatant using a lactate assay kit (Biovision #K607) according to the manufacturer’s instructions. Two female young animals and 1 male young animal per group, for a total of 6 animals, were used. Three male and 2 female older animals per group, for a total of 10 animals, were used.

MitoSOX Staining

Whole corneas were dissected and mounted with the endothelium facing up in small plastic dishes. A volume of 10 µl of 1 mM MitoSOX (#M36008, Thermo Fisher Scientific) was added on the endothelial side and incubated at room temperature for 30 minutes. The corneas were washed 3 times for 5 minutes each with 10 µl of 1 × PBS. After removing all liquid, corneas were positioned in wells of a 96-well plate and fluorescence (excitation: 510 nm, emission: 580 nm) was measured in a microplate reader. Three animals (2 female and 1 male per group) were used for both young and older animals. A total of 12 animals were used in this assay.

Fluorescein Permeability Assay

Whole corneas with sclera attached were dissected and placed in small plastic holders with the endothelial side facing upward. Ten microliters of 0.1% sodium fluorescein in bicarbonate-rich Ringer was added on the endothelial side and incubated at room temperature for 15 minutes. The corneas were washed 5 times for 5 minutes each with 10 µl bicarbonate-rich Ringer. After removing all liquid, corneas were positioned in wells of 96-well plate and fluorescence (excitation: 485 nm, emission: 520 nm) was measured in a microplate reader. Three animals (2 male and 1 female per group) were used for both young and older animals. A total of 12 animals were used in this assay.

Intraocular Pressure Measurement

By using the Tono-Pen XL (Medtronic), 6 replicate measurements were made in each eye and averaged. Intraocular pressure measurements were made in 3 animals per group (2 male and 1 female) for a total of 6 animals. The Tono-Pen XL operator was blinded to the experimental condition.

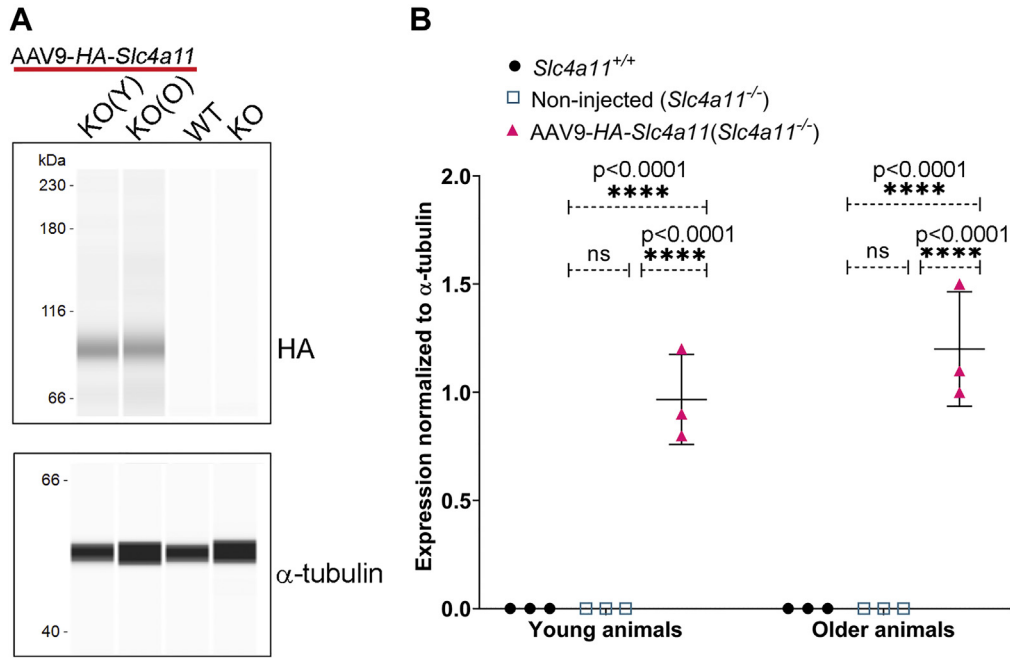


Figure 3. Transduction of AAV9-HA-*Slc4a11* into the corneal endothelium of *Slc4a11*^{-/-} (knockout [KO]) animals. **A**, Representative Wes immunoassay of corneal endothelial peelings, from *Slc4a11*^{-/-} young or older animals, KO(Y) and KO(O), respectively, 4 weeks after AAV9-HA-*Slc4a11* injections, using HA antibody. Age-matched noninjected *Slc4a11*^{+/+} (wild-type [WT]) or *Slc4a11*^{-/-} (KO) corneal endothelia were used as negative controls, α -tubulin was used as loading control. $n = 3$, 1 male and 2 female (young animals) and 2 male and 1 female (older animals). **B**, Quantification of data from **A**. Mean \pm SD. ns = not significant, $P \geq 0.1$ (1-way ANOVA with Tukey's multiple comparisons test). AAV9-HA = adeno-associated virus serotype 9 hemagglutinin.

Statistical Analysis

Error bars represent mean \pm standard deviation. For 2 groups, statistical significance was calculated using unpaired *t* tests. Analysis of variance with Tukey's multiple comparisons test was used to determine statistical significance if more than 2 groups were analyzed. Statistical analyses were conducted using GraphPad Prism software.

Model Figures

The model figures were created with the aid of [BioRender.com](https://www.biorender.com).

Results

AAV9 Vector Transduces Corneal Endothelium

In a glaucoma study, it was determined that intracameral injections of AAV9 serotype can efficiently transduce mouse corneal endothelium.¹⁹ Therefore, we decided to test whether anterior chamber injections of AAV9-GFP may be effective in our mouse model.

To determine the efficiency of AAV9 serotype transduction into the corneal endothelium, we injected the anterior chamber of 11-week-old *Slc4a11*^{-/-} animals with 0.8 μ l AAV9-GFP (3.5×10^9 Viral Genome). This dose is previously shown to be efficient in transducing the corneal endothelium.^{18,19} In vivo imaging of anesthetized mice revealed strong GFP expression in the central corneal endothelium (Fig 1A). Corneal flat mounts were stained with GFP antibody, and the number of green cells was

quantified using Image J analysis. Transduction efficiency was estimated to be $25\% \pm 12\%$ ($n = 3$, 2 male animals and 1 female animal). Cross-sections of the whole eye revealed strong GFP expression in the endothelial layer of AAV9-GFP injected animals. With GFP antibody staining, we observed nonspecific epithelial staining in both the AAV-GFP injected and the noninjected eyes. Sections with no primary antibody showed no staining (Fig 1B).

To rule out any side effects of the viral vector on corneal thickness and intraocular pressure, age-matched *Slc4a11*^{+/+} and *Slc4a11*^{-/-} animals were next injected with AAV9-GFP in 1 eye, while the other eye was not injected. Corneal thickness and intraocular pressure were measured before and 4 weeks after the procedure. No significant changes in corneal thickness were noted in *Slc4a11*^{+/+} animals between the non-injected and the injected eyes (Fig 1C). In *Slc4a11*^{-/-} mice, corneal edema was evident in both eyes before the procedure. As expected, both eyes of the KO animals showed increased corneal thickness after 4 weeks (Fig 1C). No significant changes in intraocular pressure were observed in WT and KO animals with AAV9-GFP injections (Fig 1D). Additionally, we conducted slit-lamp microscopy to determine any immune response to the injections. Although slit-lamp imaging may be considered subjective, our observations are consistent with a previous report.¹⁹ In addition, we did not observe any significant difference in corneal thickness or evidence of endothelial damage that would be indicative of inflammatory damage between injected and noninjected AAV9-GFP controls.

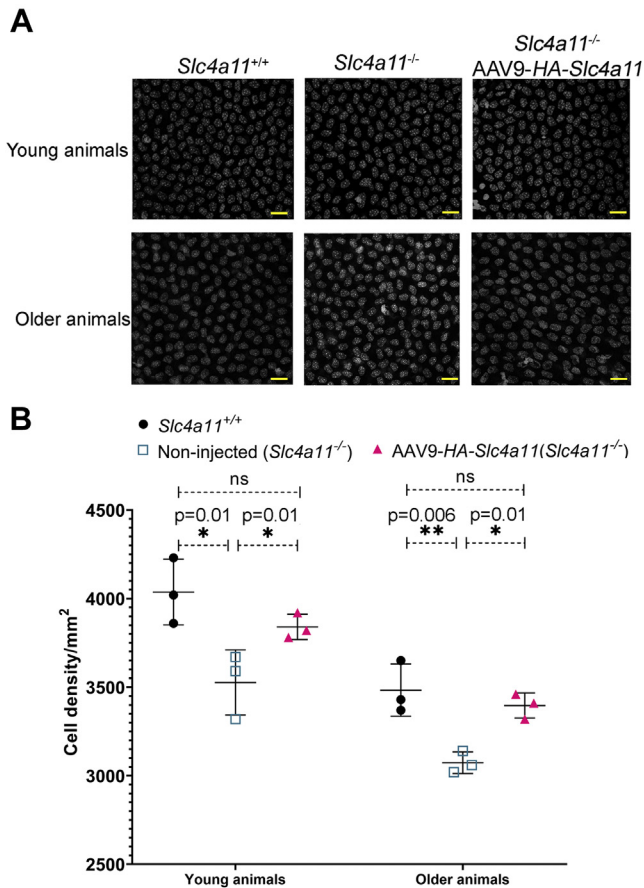


Figure 4. Decreased corneal endothelial cell loss with AAV9-HA-*Slc4a11*. **A**, Corneal endothelial cell density of young and older *Slc4a11*^{+/+}, noninjected *Slc4a11*^{-/-}, and AAV9-HA-*Slc4a11* injected *Slc4a11*^{-/-} animals visualized with DAPI staining of corneal flat mounts. Scale bar = 10 μ m. **B**, Quantification of cell density from **A**. Three animals (2 female and 1 male) were used for each group. Seven images were obtained from each group to quantify the average cell density. Mean \pm SD. *ns = not significant, $P \geq 0.1$ (1-way ANOVA with Tukey's multiple comparisons test). AAV9-HA = adeno-associated virus serotype 9 hemagglutinin.

Reduction in Corneal Edema with AAV9-HA-*Slc4a11*

The main clinical manifestations of CHED include progressive corneal edema and loss of corneal endothelial cells with age.¹ In this set of experiments, we tested whether the reintroduction of the WT allele was sufficient to reverse the disease phenotypes. Adeno-associated virus serotype 9 containing WT allele tagged with HA (AAV9-HA-*Slc4a11*) was injected into the anterior chamber of 1 eye of 5-week-old *Slc4a11*^{-/-} mice (young animals) or 11-week-old *Slc4a11*^{-/-} mice (older animals), whereas the other eye was not injected (control eyes). Mice were analyzed at 2 and 4 weeks as illustrated in [Figure S1](#) (available at www.ophtalmologyscience.org).

[Figure 2A](#) and [B](#) show that in the young KO animals, the corneal thickness was not significantly different from the age-matched WT animals at 5 weeks of age (0 day of the injection). A significant increase in corneal thickness was noted in

the KO animals' noninjected eyes 4 weeks later. However, the AAV9-injected eyes showed less increase in corneal thickness compared with the noninjected eyes. In the older group, increased corneal thickness was evident in the KO animals at week 11 before injection ([Fig 2C, D](#)). With AAV9-HA-*Slc4a11* injection, corneal edema did not increase significantly at week 4 compared with week 0 post-injection. However, in the noninjected eye, the cornea continued to thicken with time ([Fig 2C, D](#)).

Slc4a11 Transduction

Corneal endothelial peelings were isolated 4 weeks after AAV9 injection, and Wes immunoassay was conducted to determine the presence of the HA tag. The molecular weight of *Slc4a11* is approximately 100 kDa.⁶ Expression of HA in this molecular weight range was detected in the AAV-injected eyes ([Fig 3A, B](#)), but not in the noninjected WT or KO corneal peelings. Because *Slc4a11* antibodies were not used to measure the transduction efficiency, determining whether the protein expression in the injected eyes was comparable to the WT corneal endothelium was not possible.

Decreased Loss of Corneal Endothelial Cell Density

To measure corneal endothelial cell density, animals were euthanized at week 4, and the corneal cups were stained with DAPI to visualize nuclei. Image J analysis was conducted to count the number of nuclei in the corneal endothelium using Particle Analysis macro. [Figure 4A](#) and [B](#) show that endothelial cell density was approximately 12% lower in KO animals at both 9 and 15 weeks of age relative to WT. Both young and older animals injected with AAV9-HA-*Slc4a11* showed less endothelial cell loss with densities slightly, but not significantly, lower than WT.

Anterior chamber injections are stressful to the mice, and when both eyes were injected, the animals often died of the stress. Thus, only 1 eye in each mouse belonging to the control and experimental groups were injected. We decided to inject AAV-CAG-Null separately into another group of animals to control for any off-target effects from the virus vector. One eye of 11-week-old *Slc4a11*^{-/-} animals was injected, and the other eye was left noninjected. Corneal thickness ([Fig S2A, B](#)) and corneal endothelial densities ([Fig S2C, D](#)) were comparable between the virus-injected and noninjected eyes.

Reduction in Stromal Lactate Levels and Increase in Lactate Transporter Expression with AAV9-HA-*Slc4a11*

In *Slc4a11*^{-/-} animals, reduction in corneal endothelial pump function leads to corneal edema.²⁰ Depressed pump function results from reduced lactate efflux from the cornea leading to the accumulation of lactate in the stroma,²¹ which progresses with age in the *Slc4a11* KO.²⁰ Lactate transporters, MCT1, 2, and 4, are active in the corneal endothelium,²¹⁻²³ and their functions are crucial in the maintenance of corneal deturgescence¹ ([Fig 5A](#)). [Figure 5B](#)

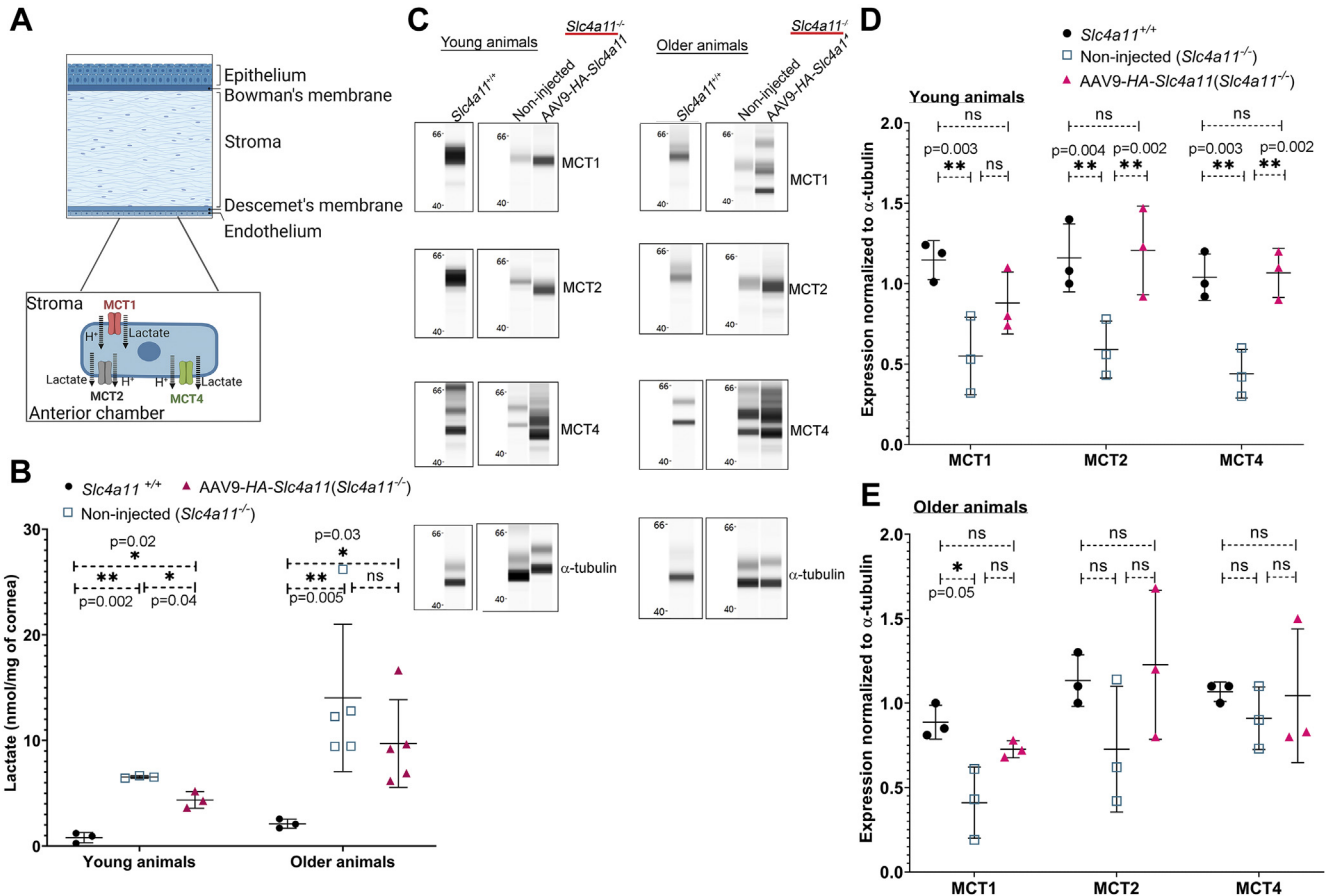


Figure 5. Lactate levels are reduced and lactate transporter expressions are increased with AAV9-*HA-Slc4a11* in young animals. **A**, Schematic of the corneal layers and a diagram of lactate movement from the cornea into the anterior chamber with the aid of lactate transporters, monocarboxylate transporter (MCT)1, 2, and 4.^{1,23} **B**, Quantification of lactate levels in *Slc4a11*^{-/-} animals. n = 3 (young animals, 2 female and 1 male for each group), n = 5 (older animals, 3 male and 2 female for each group). Mean ± SD. ns = not significant, $P \geq 0.1$ (1-way ANOVA with Tukey's multiple comparisons test). **C**, Representative Wes immunoassay of young and older animals for lactate transporters MCT1, MCT2, MCT4, and loading control α -tubulin. **D**, Quantification of Wes immunoassay results from young animals. n = 3, 1 male and 2 females per group. ns = not significant, $P \geq 0.1$ (1-way ANOVA with Tukey's multiple comparisons test). **E**, Quantification of Wes immunoassay results from older animals. n = 3, 2 males and 1 female per group. ns = not significant, $P = 0.05$. For MCT1, the band closest to 66 KDa was used for quantification. Lower molecular weight band was used for MCT4 quantification. AAV9-HA = adeno-associated virus serotype 9 hemagglutinin; MCT = monocarboxylate transporter.

shows that concomitant with corneal thickness changes, AAV9-*HA-Slc4a11* injection caused a 30% reduction in corneal [lactate] in young animals. In the older animals, which started with higher [lactate], a small but statistically insignificant decrease in [lactate] was observed. As the [lactate] reduced with AAV9-*HA-Slc4a11* injection, we next determined whether lactate transporters' protein expression was affected with the introduction of *Slc4a11*. In the young animals, slight upregulation of MCT1 and 2 protein levels was observed (Fig 5C, D); however, MCT4 expression increased significantly with AAV9-*HA-Slc4a11* injection (Fig 5C, D). In the older animals, lactate transporter expressions were elevated with the introduction of the AAV, but these levels were not significantly improved from those observed in noninjected eyes (Fig 5C, E).

AAV9-*HA-Slc4a11* Injection Improves Endothelial Morphology and Barrier

Cell membrane integrity is essential for the normal functioning of the endothelial pump. The shape and organization of corneal endothelial cells are aberrant in CHED.^{5,24} A recent study from our laboratory has revealed abnormal cytoskeletal structure of the corneal endothelium with the loss of *Slc4a11*.⁹ To assess the cytoskeleton, corneal flat mounts were stained with phalloidin to visualize the F-actin network. With AAV9-*HA-Slc4a11*, the phalloidin staining pattern appeared more organized in both young and older animals when compared with noninjected controls (red ellipses in Fig 6A). Moreover, the phalloidin fluorescence intensities of the AAV injected eyes were comparable to that of WT in the young animals (Fig 6B).

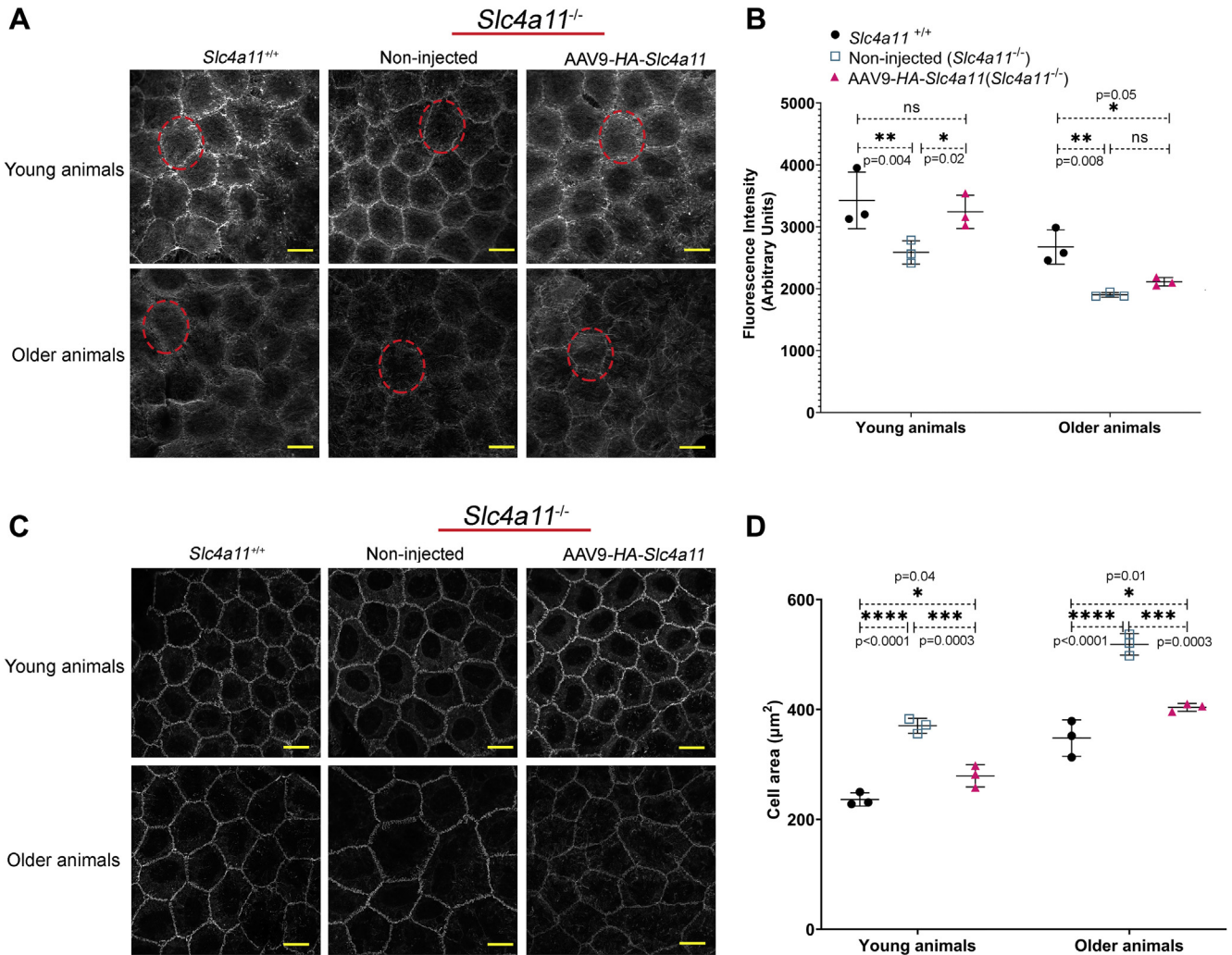


Figure 6. Cytoskeletal structure and tight junction architecture are improved with AAV9-HA-*Slc4a11*. **A**, Phalloidin staining of corneal endothelia to visualize F-actin cytoskeleton network in *Slc4a11^{+/+}*, noninjected *Slc4a11^{-/-}* and AAV9-HA-*Slc4a11* injected *Slc4a11^{-/-}* animals. **B**, Quantification of fluorescence intensity of phalloidin staining. **C**, ZO-1 staining of the corneal endothelia to visualize tight junction structure in *Slc4a11^{+/+}*, noninjected *Slc4a11^{-/-}* and AAV9-HA-*Slc4a11* injected *Slc4a11^{-/-}* animals. **D**, Quantification of cell area. **B** and **D**, Three animals (2 females and 1 male) were used for each group. Seven images were obtained from each group to quantify the average cell density. Mean \pm SD. * $P < 0.05$, ** $P < 0.01$, *** $P < 0.001$, **** $P < 0.0001$. ns = not significant (1-way ANOVA with Tukey's multiple comparisons test). AAV9-HA = adeno-associated virus serotype 9 hemagglutinin.

Endothelial cells express the tight junction protein ZO-1.²⁵ The expression pattern of ZO-1 is incomplete, which accounts for a weak endothelial barrier that allows the passage of nutrients and other molecules into the stroma.² Increased cell size is observed in *Slc4a11* KO corneal endothelium.^{5,9} To assess cell size, corneal cups were stained with ZO-1. In the young noninjected eyes, the endothelial cells appeared larger when compared with WT cells. In the older animals, cell area was significantly altered between WT and KO animals. The AAV9-HA-*Slc4a11* injections improved the cell area in *Slc4a11^{-/-}* young and older animals (Fig 6C, D).

Paracellular permeability of endothelial cells was measured using fluorescein penetration of the endothelium. Figure 7A shows that KO endothelium has significantly higher fluorescein penetration consistent with a

dysfunctional barrier function. With AAV9-HA-*Slc4a11* injection, fluorescein permeability of the endothelium was significantly reduced in young animals. Small but significant improvement was also observed between noninjected and AAV9-HA-*Slc4a11* injected eyes of older animals.

Oxidative Stress

Loss of *Slc4a11* is associated with mitochondrial oxidative stress.⁶ To determine whether AAV9-HA-*Slc4a11* injection reduces reactive oxygen species (ROS) levels, we stained the corneal cups with mitochondria superoxide marker, MitoSOX. Quantification of fluorescence intensity revealed significant reduction in ROS levels in young animals and a small but not statistically significant

increased [lactate] in the cornea.^{20,21} With AAV9-*HA-Slc4a11* injection, concomitant with reduced edema, we observed a significant reduction of [lactate] in the young KO animal eyes compared with noninjected KO eyes. In the older animals, consistent with minimal improvement in corneal thickness, there was a small but not significant reduction in [lactate]. Supporting these observations, the expression of the major lactate transporters in the corneal endothelium increased with AAV9-*HA-Slc4a11* in young animals but less in older animals.

Endothelial pump function relies on both lactate transport and an intact osmotic barrier.^{20,21} Changes in cell shape in *Slc4a11* KO corneal endothelium have been reported.⁹ In *Slc4a11* KO corneal endothelial cells, aberrations in actin cytoskeleton assembly, tight junction organization, cell shape changes, and increased paracellular permeability were observed.⁹ In young animals, AAV9-*HA-Slc4a11* introduction restored all of these changes to the levels comparable to those observed in WT animals. However, older animals showed little improvement in these parameters.

Our data show that AAV9-*HA-Slc4a11* introduction into the anterior chamber can reverse the major disease phenotype associated with CHED. It is a viable option that can bypass invasive treatments such as corneal transplantation. Furthermore, we show that AAV9 transduction into the corneal endothelium does not affect intraocular pressure or cause inflammation, indicating a safe treatment alternative. Finally, we provide evidence that the gene therapy avenue is most effective during the initial stages of the disease and has limited potential once the structural integrity of the corneal endothelial layer or stroma is significantly affected.

Oxidative stress is likely the cause of the altered gene expression and paracellular permeability because

quenching ROS can reduce corneal edema.^{6,29} Consistent with this notion, we found that reintroduction of *Slc4a11* reduces mitochondrial superoxide levels within the endothelium. This suggests that ROS quenching can temporarily preserve cell function until gene replacement is achieved. Mutations in *Slc4a11* are the most common cause of CHED.³⁰ Congenital hereditary endothelial dystrophy is common among people in India, Saudi Arabia, and Iran. Several studies have shown that approximately 100% of the CHED patients had mutations in *Slc4a11*.^{31–33} There are several *Slc4a11* mutations associated with CHED.^{8,31,34} The approach in human patients could be via a CRISPR repair of the mutation or overexpression of WT *Slc4a11* as done here. The latter approach may be limited by dominant negative associations.³⁵ In any approach, therapy must start at the earliest stage possible before cell loss and structural changes become irreversible. One of the limitations of our study is the low transduction efficiency of the corneal endothelium with the AAV9 serotype. Future studies may use different AAV serotypes to improve this, which may lead to the improvement of disease-associated symptoms in older animals. As done previously,¹⁹ we conducted slit-lamp imaging to determine any signs of inflammation. Future studies may consider immunostaining for macrophages in corneal sections to rule out any inflammation from AAV injections.

Acknowledgments

The authors thank Dr. Shimin Li for support and expert advice and Dr. Catherine Cheng for the use of Protein Simple Wes system and Zeiss LSM 800 confocal microscope.

Footnotes and Disclosures

Originally received: August 2, 2021.

Final revision: October 29, 2021.

Accepted: November 15, 2021.

Available online: November 23, 2021. Manuscript no. D-21-00137

Vision Science Program, School of Optometry, Indiana University Bloomington, Bloomington, Indiana.

Disclosure(s):

All authors have completed and submitted the ICMJE disclosures form.

The author(s) have no proprietary or commercial interest in any materials discussed in this article.

Financial Support: R01EY031321 (J.A.B.) and R01EY008834 (J.A.B.), National Institutes of Health/National Center for Advancing Translational Sciences CTSI TL1 TR002531 and UL1 TR002529 (2018-2020) (R.S.), and Knights Templar Eye Foundation career starter grant (2019-2021) (R.S.). The funding organizations had no role in the design or conduct of this research.

HUMAN SUBJECTS: Human subjects were not included in this study. All animal experiments were conducted in accordance with institutional guidelines and the current regulations of the National Institutes of Health, the United States Department of Health and Human Services, the United States Department of Agriculture, and the Association for Research in Vision and Ophthalmology (ARVO) Statement for the Use of Animals in

Ophthalmic and Vision Research. All research adhered to the tenets of the Declaration of Helsinki. Individual patient-level consent was not required.

Author Contributions:

Conception and design: Shyam, Ogando, Bonanno

Data collection: Shyam, Ogando, Kim, Murugan, Choi

Analysis and interpretation: Shyam, Ogando, Kim, Murugan, Bonanno

Obtained funding: Shyam, Bonanno; Study was performed as part of the authors' regular employment duties. No additional funding was provided.

Overall responsibility: Shyam, Ogando, Kim, Murugan, Choi, Bonanno

Abbreviations and Acronyms:

AAV = adeno-associated virus; **AAV9** = adeno-associated virus serotype 9; **CAG** = chicken β -actin; **CHED** = congenital hereditary endothelial dystrophy; **GFP** = green fluorescent protein; **HA** = hemagglutinin; **KOSlc4a11^{-/-}** = knockout; **MCT** = monocarboxylate transporter; **PBS** = phosphate-buffered saline; **WTSlc4a11^{+/+}** = wild-type; **ZO-1** = zonula occludens 1.

Keywords:

Adeno-associated virus, Congenital hereditary endothelial dystrophy, Endothelial dystrophy, Gene therapy.

Correspondence:

Rajalekshmy Shyam, PhD, 800 E. Atwater Avenue, Indiana University School of Optometry, Bloomington, IN 47402. E-mail: rashyam@iu.edu.

References

1. Bonanno JA. Molecular mechanisms underlying the corneal endothelial pump. *Exp Eye Res.* 2012;95:2–7.
2. Bourne WM. Biology of the corneal endothelium in health and disease. *Eye.* 2003;17:912–918.
3. Vanathi M, Panda A, Vengayil S, et al. Pediatric keratoplasty. *Surv Ophthalmol.* 2009;54:245–271.
4. Vithana EN, Morgan P, Sundaresan P, et al. Mutations in sodium-borate cotransporter SLC4A11 cause recessive congenital hereditary endothelial dystrophy (CHED2). *Nat Genet.* 2006;38:755–757.
5. Han SB, Ang H-P, Poh R, et al. Mice with a targeted disruption of Slc4a11 model the progressive corneal changes of congenital hereditary endothelial dystrophy. *Invest Ophthalmol Vis Sci.* 2013;54:6179–6189.
6. Ogando DG, Choi M, Shyam R, et al. Ammonia sensitive SLC4A11 mitochondrial uncoupling reduces glutamine induced oxidative stress. *Redox Biol.* 2019;26:101260.
7. Guha S, Chaurasia S, Ramachandran C, Roy S. SLC4A11 depletion impairs NRF2 mediated antioxidant signaling and increases reactive oxygen species in human corneal endothelial cells during oxidative stress. *Sci Rep.* 2017;7:4074.
8. Aldave AJ, Han J, Frausto RF. Genetics of the corneal endothelial dystrophies: an evidence-based review. *Clin Genet.* 2013;84:109–119.
9. Ogando DG, Shyam R, Kim ET, et al. Inducible Slc4a11 knockout triggers corneal edema through perturbation of corneal endothelial pump. *Investig Ophthalmology Vis Sci.* 2021;62:28.
10. Li S, Shyam R, Ogando DG, Bonanno JA. Bicarbonate activates glycolysis and lactate production in corneal endothelial cells by increased pHi. *Exp Eye Res.* 2020;199:108193.
11. Busin M. Descemet-stripping automated endothelial keratoplasty for congenital hereditary endothelial dystrophy. *Arch Ophthalmol.* 2011;129:1140.
12. Tan DT, Dart JK, Holland EJ, Kinoshita S. Corneal transplantation. *Lancet.* 2012;379:1749–1761.
13. de By TMMH. Shortage in the face of plenty: Improving the allocation of corneas for transplantation. In: *Adequate HLA Matching in Keratoplasty*. Basel: Karger; 2002:56–61. <https://www.karger.com/Article/Abstract/67656>.
14. Fuest M, Yam GH-F, Mehta JS, Duarte Campos DF. Prospects and challenges of translational corneal bioprinting. *Bioengineering.* 2020;7:71.
15. Borrás T, Xue W, Choi VW, et al. Mechanisms of AAV transduction in glaucoma-associated human trabecular meshwork cells. *J Gene Med.* 2006;8:589–602.
16. Barker SE, Broderick CA, Robbie SJ, et al. Subretinal delivery of adeno-associated virus serotype 2 results in minimal immune responses that allow repeat vector administration in immunocompetent mice. *J Gene Med.* 2009;11:486–497.
17. Uehara H, Zhang X, Pereira F, et al. Start codon disruption with CRISPR/Cas9 prevents murine Fuchs' endothelial corneal dystrophy. *Elife.* 2021;10.
18. Bastola P, Song L, Gilger BC, Hirsch ML. Adeno-associated virus mediated gene therapy for corneal diseases. *Pharmaceutics.* 2020;12:767.
19. O'Callaghan J, Crosbie DE, Cassidy PS, et al. Therapeutic potential of AAV-mediated MMP-3 secretion from corneal endothelium in treating glaucoma. *Hum Mol Genet.* 2017;26:1230–1246.
20. Li S, Kim E, Ogando DG, Bonanno JA. Corneal endothelial pump coupling to lactic acid efflux in the rabbit and mouse. *Invest Ophthalmology Vis Sci.* 2020;61:7.
21. Li S, Kim E, Bonanno JA. Fluid transport by the cornea endothelium is dependent on buffering lactic acid efflux. *Am J Physiol Physiol.* 2016;311:C116–C126.
22. Li S, Nguyen TT, Bonanno JA. CD147 required for corneal endothelial lactate transport. *Investig Ophthalmol Vis Sci.* 2014;55:4673–4681.
23. Nguyen TT, Bonanno JA. Lactate-H⁺ transport is a significant component of the in vivo corneal endothelial pump. *Invest Ophthalmology Vis Sci.* 2012;53:2020.
24. Feizi S. Corneal endothelial cell dysfunction: etiologies and management. *Ther Adv Ophthalmol.* 2018;10, 251584141881580.
25. Schmedt T, Silva MM, Ziaei A, et al. Molecular bases of corneal endothelial dystrophies. *Am J Pathol.* 2010;95:24–34.
26. Liu C, Ogando D, Bonanno JA. SOD2 contributes to anti-oxidative capacity in rabbit corneal endothelial cells. *Mol Vis.* 2011;17:2473–2481.
27. Pierce EA, Bennett J. The status of RPE65 gene therapy trials: safety and efficacy. *Cold Spring Harb Perspect Med.* 2015;5:a017285.
28. Petit L, Khanna H, Punzo C. Advances in gene therapy for diseases of the eye. *Hum Gene Ther.* 2016;27:563–579.
29. Shyam R, Ogando DG, Choi M, et al. Mitochondrial ROS induced lysosomal dysfunction and autophagy impairment in an animal model of congenital hereditary endothelial dystrophy. *Investig Ophthalmology Vis Sci.* 2021;62:15.
30. Patel SP, Parker MD. SLC4A11 and the pathophysiology of congenital hereditary endothelial dystrophy. *Biomed Res Int.* 2015;2015:1–7.
31. Aldahmesh MA, Khan AO, Meyer BF, Alkuraya FS. Mutational spectrum of SLC4A11 in autosomal recessive CHED in Saudi Arabia. *Invest Ophthalmol Vis Sci.* 2009;50:4142–4145.
32. Moazzeni H, Javadi MA, Asgari D, et al. Observation of nine previously reported and 10 non-reported SLC4A11 mutations among 20 Iranian CHED probands and identification of an MPDZ mutation as possible cause of CHED and FECD in one family. *Br J Ophthalmol.* 2020;104:1621–1628.
33. Hemadevi B. Identification of mutations in the SLC4A11 gene in patients with recessive congenital hereditary endothelial dystrophy. *Arch Ophthalmol.* 2008;126:700.
34. Kao L, Azimov R, Shao XM, et al. Multifunctional ion transport properties of human SLC4A11: comparison of the SLC4A11-B and SLC4A11-C variants. *Am J Physiol Cell Physiol.* 2016;311:C820–C830.
35. Malhotra D, Loganathan SK, Chiu AM, et al. Human corneal expression of SLC4A11, a gene mutated in endothelial corneal dystrophies. *Sci Rep.* 2019;9:9681.